Copy No. 10

NASA PROGRAM APOLLO WORKING PAPER NO. 1156

RESULTS OF TWO ONE-QUARTER SCALE APOLLO MODEL IMPACT TESTS UTILIZING DIFFERENT IMPACT ATTENUATION SYSTEMS

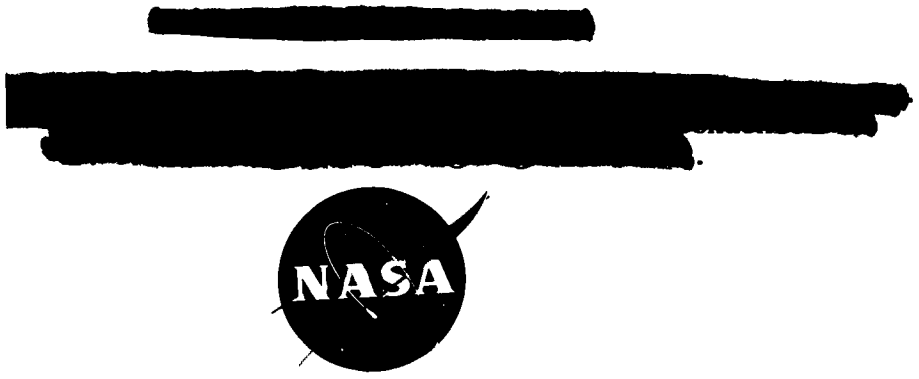

NATIONAL AERONAUTICS AND SPACE ADMINISTRATION
MANNED SPACECRAFT CENTER
Houston, Texas

January 29, 1965

NASA PROGRAM APOLLO WORKING PAPER NO. 1156

RESULTS OF TWO ONE-QUARTER SCALE APOLLO MODEL IMPACT TESTS UTILIZING DIFFERENT IMPACT ATTENUATION SYSTEMS

Prepared By: Harold E. Benson

Harold E. Benson
Head, Landing Dynamics Section

Robert B. West
Manager, Earth Landing Subsystem

Authorized for Distribution:

Warren Gillespie, Jr.
for Maxime A. Faget
Assistant Director for
Engineering and Development

NATIONAL AERONAUTICS AND SPACE ADMINISTRATION

MANNED SPACECRAFT CENTER

HOUSTON, TEXAS

January 29, 1965

TABLE OF CONTENTS

Page

SUMMARY 1

INTRODUCTION 2

APPARATUS AND PROCEDURE 3

- Models 3
- Heat Shields 3
- Struts 4
- Instrumentation 4
- Photographic Data 4
- Test Procedure 5

RESULTS OF TESTS 5

- Angular Accelerations 5
- Normal Accelerations 6
- Longitudinal Accelerations 7
- Acceleration Histories 8
- Stability 8

REMARKS 9

CONCLUSIONS 10

REFERENCES 11

TABLE I 12

FIGURES 13

LIST OF FIGURES

Figure No.		Page
1	General arrangement of one-quarter-scale dynamic Apollo model with no impact attenuation struts . . .	13
2	General arrangement of one-quarter-scale dynamic Apollo model incorporating impact attenuation struts	14
3	Heat shield force-deflection and test setup	15
4	Sketches of vertical and horizontal shock struts . .	16
5	Force-deflection curves for the oleo and honeycomb struts	17
6	Model on support carriage	18
7	Definition of axes, accelerations and attitudes . . .	19
8	Strut model angular accelerations	20
9	No strut model angular accelerations	21
10	Strut model normal accelerations	22
11	No strut model normal accelerations	23
12	Strut model longitudinal accelerations	24
13	No strut model longitudinal accelerations	25
14	Typical acceleration histories for strut model . . .	26
15	Typical acceleration histories for the no strut model	27
16	Typical impact depressions	28

RESULTS OF TWO ONE-QUARTER SCALE APOLLO MODEL IMPACT TESTS

UTILIZING DIFFERENT IMPACT ATTENUATION SYSTEMS

By Harold E. Benson and Robert B. West
Manned Spacecraft Center

SUMMARY

Experimental model investigations were conducted to obtain preliminary data on the landing impact accelerations and stability characteristics of the Apollo command module. Two one-quarter scale dynamic models of the Apollo vehicle were utilized in the course of this investigation. The models included one with a fiberglas heat shield attached directly to the model and one with a similar heat shield attached to the model by impact-attenuation struts. Accelerometers were installed in both models to measure the vertical, longitudinal, transverse, and angular accelerations. The tests consisted of impacting the models at equivalent horizontal velocities from 0 to 50 ft/sec at a constant equivalent vertical velocity of 30 ft/sec and at pitch attitudes, in increments of 5°, from -20° to +20° or to the attitude which, if exceeded, resulted in the model turning over. Within the above test parameters, the impact stability limits for the no-strut model was approximately 19° positive pitch at an equivalent full-scale horizontal velocity (V_H) of 15 ft/sec and 5° positive pitch at V_H of 50 ft/sec. The stability limits for the strut model were determined to be approximately 17° positive pitch at V_H of 30 ft/sec and 13° positive pitch at V_H of 50 ft/sec. The maximum accelerations recorded with the no-strut model were as follows:

1. Normal accelerations, 112g at 15 fps V_H and 5° negative pitch

2. Longitudinal accelerations, 33g at 30 fps V_H and 4° negative pitch

3. Angular accelerations, 21.2g/ft at 40 fps V_H and 2° positive pitch

The maximum accelerations recorded with the strut model were as follows:

1. Normal accelerations, 19.7g at 0 fps V_H and 0° pitch

2. Longitudinal accelerations, 19g at 50 fps V_H and 8° negative pitch

3. Angular accelerations, 6.7g/ft at 40 fps V_H and 15° positive pitch

No attempt will be made in this paper to predict specific results which will be obtained from the full-scale spacecraft impact tests; however, it can be assumed that the above results obtained from the no-strut model will be higher than the results obtain from the full-scale spacecraft. This can be expected since the model experienced very little strain and no structural failure as compared to what might be expected to occur with the full-scale vehicle. The data obtained from the strut model will more closely represent a full-scale spacecraft employing a similar impact attenuation system since the majority of the impact energy is absorbed through the struts.

INTRODUCTION

A program of tests of one-quarter scale dynamic models of the Apollo command module was initiated to supplement full-scale impact testing of the command module. The purpose of this program was to establish critical test parameters for use in full-scale tests. The model program also served as a means of conducting tests under extreme conditions which might not be feasible to investigate with full-scale vehicles. The specific objectives of the test program were to provide preliminary data on the landing impact accelerations and stability characteristics of the Apollo vehicle. The test conditions were within the range of landing velocities and impact attitudes which have been defined as the design limits for the Apollo command module.

Of the two models tested, one consisted of a solid balsa model with an elastically scaled fiberglas heat shield bonded to the bottom of the model. The second model consisted of a less stiff configuration, incorporating an identical heat shield as used on the solid balsa model, but with the heat shield attached through a series of oleo and crushable aluminum honeycomb struts. This report will discuss in detail the test program, the models tested, and the results obtained from each of the two models.

APPARATUS AND PROCEDURE

The one-quarter scale dynamic model tests were conducted at the Langley Research Center (LRC). The models were launched as free bodies and were impacted in dry sand. This sand was standard Ottawa Silica Sand 20-30 A.S.T.M. Designation C-190, C-1 of the American Society for Testing Materials.

Models

Two dynamically similar models were utilized in this test program. They consisted of a no-strut model, as illustrated in figure 1, and a less stiff model incorporating impact attenuation struts, as shown in figure 2. The no-strut model was constructed at the Langley Research Center and consisted of a solid-balsa command module (CM) with a fiberglas heat shield bonded directly to the bottom of the model. The strut model was constructed by North American Aviation (NAA) (ref. 1) and consisted of a fiberglas shell with an internal structure of two aluminum webs and nine vertical aluminum tee section ribs. Laminated balsa was incorporated in the bottom of the model. Hardwood blocks were embedded in the balsa on both models for mounting the accelerometers. The NAA model was initially tested in two configurations. In one configuration, the heat shield was supported by six near-vertical oleo struts and eight lateral support struts containing cores of precrushed aluminum honeycomb. In a second configuration, the struts were removed and the heat shield was attached directly to the bottom of the CM. High frequency vibrations in this second configuration prevented an accurate interpretation of the accelerometer records and hence no data from this model are presented.

Heat Shields

The heat shields used in these tests were constructed of Styrofoam sandwiched between face sheets of laminated fiberglas. They were designed to have an EI (modulus of elasticity $\times$ moment of inertia) equal to 2.5 times the EI of the spacecraft heat shield. Prior to making the drop tests, force-deflection tests were conducted on each of the heat shields as illustrated in figure 3. Each heat shield was loaded to 1500 pounds, or to a maximum deflection of 0.25 in., whichever occurred first. The load was applied through a 4 $\times$ 4-in. block located at the center of the heat shield. A typical force-deflection curve from one of these tests is presented in figure 3.

Struts

The oleo shock-absorbing struts and the aluminum honeycomb shock-absorbing struts are illustrated in figure 4. The general arrangements of these struts between the CM and the heat shield is presented in figure 2. The hydraulic fluid utilized in the oleo struts consisted of a mixture of 80 percent ethylene glycol and 20 percent water. A typical load-stroke curve, for the oleo strut, is shown in figure 5a. The horizontal shock-strut contained a core of aluminum honeycomb, Hexel Alloy 3003-819, precrushed from 0.625 to 0.5 in. The honeycomb cell size was 0.1875 in. and the wall thickness was 0.003 in. The diameter of the core was 1.1 in. A typical load-stroke curve for the aluminum strut is illustrated in figure 5b. The curves of figure 5 were provided by NAA.

Instrumentation

The models were instrumented with strain-gage accelerometers mounted on hardwood blocks which were potted into the balsa wood. Linear accelerations at the center of gravity in the X and Z directions and angular accelerations about the Y-axis were measured. The accelerometer mounted on the strut model had a capacity of ±100g along the X-axis, ±50g along the Z-axis, and ±12.5g/ft angular acceleration about the Y-axis. (Note: Angular acceleration measured in g/ft is the tangential acceleration per ft measured from the Y-axis.) The accelerometers mounted on the no-strut model had a capacity of ±100g along the X-axis, ±50g along the Z-axis, and ±50g/ft angular acceleration about the Y-axis. The signals from the accelerometers were transmitted through cables to the amplifying and recording equipment.

Photographic Data

Model contact attitudes, rotations and displacements after contact were determined from high speed motion pictures. This photographic coverage was obtained from three stationary and two panning cameras. Two of the stationary cameras provided a three-quarter frontal view with the cameras operating at shutter speeds of 128 and 64 frames per sec. The third stationary camera, which was situated so as to provide a side view of the model at impact, was operated at a shutter speed of 128 frames per sec. The two panning cameras were mounted near the point of impact and were operated at shutter speeds of 48 and 200 frames per sec.

Test Procedure

The tests were conducted by releasing the models from a pendulum-supported carriage, illustrated in figure 6, and allowing them a free-fall from the height required to obtain an equivalent full-scale vertical velocity of 30 ft/sec. The true velocities at which the models were tested were determined by the scale relationship shown in table I. The desired horizontal velocity was obtained by adjusting the amplitude of swing of the pendulum from which the carriage was released. The model release mechanism, which consisted of an Air Force MA-4A aircraft bomb rack, was actuated at the bottom of the swing by interrupting a light beam to a photo-electric cell. The carriage was capable of producing an equivalent full-scale horizontal velocity of 50 ft/sec with the model impacting at an equivalent vertical velocity of 30 ft/sec. The pitch attitude of the model about the Y-axis could be varied in 5° increments from +20° to -20° and the carriage could be rotated to roll attitudes of 90° and 180°. The sand, into which the models were impacted, was contained in a box 6 ft wide, 36 ft long, and 6 in. deep. The box had a plywood bottom which rested on a concrete floor. Prior to each drop, the sand was loosened and smoothed to a uniform depth of 6 in.

RESULTS OF TESTS

The axes, accelerations, and model attitudes used in this investigation are defined in figure 7.

The test results obtained from the strut model and the no-strut model are presented in figures 8 through 13, which show the accelerations at various pitch attitudes and equivalent horizontal velocities. The figures present the vertical and longitudinal accelerations measured at the center of gravity and the angular accelerations about the Y-axis. Oscillograph records of typical acceleration histories are reproduced in figures 14 and 15. Figure 16 shows a comparison of the impact depressions and the distances the two models slid after impact. The impact depressions presented are from tests conducted at equivalent horizontal velocities of 0 to 50 ft/sec and pitch attitudes of 0°, or the negative pitch attitude nearest to 0° that was obtainable. Drop weights and moments of inertia are presented in table I.

Angular Accelerations

The angular accelerations obtained with the strut model ranged from +4g/ft to -6.6g/ft and are presented in figure 8. The highest

angular acceleration of -6.6g/ft was recorded at a horizontal velocity of 40 ft/sec and a positive impact attitude of 15°. The model was unstable under this condition and it turned over. As determined from previous test programs, and discussed in reference 2, a negative pitch attitude at impact produces an initial counterclockwise or positive rotation and a positive impact attitude produces a clockwise rotation. At negative impact attitudes, this model rotated first in a counterclockwise direction and then in a clockwise direction which resulted in a reversal of the angular accelerations. These secondary accelerations at times exceeded the initial accelerations as indicated in figure 8 by the flagged test points. The minimum time for reversal of peak accelerations was determined to be approximately 0.005 seconds (0.01 seconds full-scale) which occurred at a horizontal velocity of 15 ft/sec and an attitude of -10°. This reversal occurred between -1.4g/ft and +3g/ft. A limited number of tests were conducted with the center of gravity displaced at 90° and 180° about the X-axis with respect to the direction of flight. No significant changes in motion occurred under these conditions and the angular accelerations obtained are presented in figure 8.

The angular accelerations recorded with the no-strut model, as shown in figure 9, ranged from +10.2g/ft to -21.2g/ft. The highest angular acceleration of -21.2g/ft was recorded at a horizontal velocity of 40 ft/sec and a positive impact attitude of 2°. The model was unstable under these conditions. The motions with respect to impact attitudes were similar to those described for the strut model. The minimum time for reversal of peak accelerations was determined to be approximately 0.003 sec (0.006 sec full-scale) which occurred at a horizontal velocity of 15 ft/sec and an attitude of -7°. This reversal occurred during slideout between -1.5g/ft and +2.6g/ft.

Normal Accelerations

The normal accelerations recorded with the strut model are presented in figure 10. The highest normal acceleration obtained with this model was 19.8g at zero horizontal velocity and 0° impact attitude. The struts were designed to limit the accelerations to a maximum of 20g in the normal direction and it is noted from this figure that the data obtained are close to this design condition. In general, the data follow a slight curve with the maximum accelerations occurring at 0° impact attitude and decreasing slightly as the impact angle increases in the positive and negative direction. The range of normal accelerations varied in the tests from 11 to 20g. It is of interest to note that with roll orientations of 90° and 180°, the normal accelerations are slightly higher than with zero roll displacements. This result may be due to the fact that the strut system was not designed for impacts at other than 0° roll orientation.

The normal accelerations recorded with the no-strut model are presented in figure 11. The highest normal acceleration obtained with this model was 112g at a horizontal velocity of 15 ft/sec and a negative impact attitude of 5°. The general data pattern again tends to follow a curve, with the peak near the -5° impact attitude and the magnitude decreasing as the impact angles change in either direction from this attitude. The lowest acceleration recorded with the no-strut model was 32g which occurred at an extremely high negative impact attitude of 25° and a horizontal velocity of 15 ft/sec. Correspondingly low accelerations also occurred at a positive impact attitude of 14° and a horizontal velocity of 15 ft/sec. The accelerations acting along the X-axis, designated as normal accelerations, are reduced to some extent with an increase in the angle of impact since these accelerations represent only a component of the total acceleration. In addition, two other factors which tend to reduce the normal accelerations are the penetration of the model into the sand and the angular rotation of the model. With positive attitudes, the g loading is reduced due to the pitching or rocking of the model (ref. 3). At higher negative attitudes, the model achieves better penetration of the sand and dissipation of energy. For example, at -25° and 15 ft/sec, the initial sand penetration was 1.94 in. and the angular acceleration was 33g whereas at +14° and 15 ft/sec the initial sand penetration was 0.875 in. and the angular acceleration was 51g. Both of these impact conditions produced essentially the same normal accelerations.

Longitudinal Accelerations

The longitudinal accelerations for the strut model are presented in figure 12. The highest longitudinal acceleration obtained with this model was +19g at a horizontal velocity of 50 ft/sec and impact attitude of -8°. It can be noted from figure 12 that longitudinal acceleration reversals occur when the model impacted at positive pitch attitudes. At initial impact, the longitudinal accelerations were negative as the vertical velocity was dissipated. Acceleration reversal took place as the model rotated about the heat shield and the longitudinal accelerations become positive as the horizontal velocity was dissipated. The minimum time for reversal of the peak longitudinal accelerations was approximately 0.012 sec (0.024 sec full-scale) which occurred at a horizontal velocity of 15 ft/sec and a positive impact attitude of 10°. These accelerations ranged from -5g to +8g. The accelerations for the 90° roll-oriented attitude, defined as transverse to the Z-axis, are not shown, but were determined to be of the order of 10 to 15g. The longitudinal accelerations which correspond with these accelerations were between 4 and 5g as shown in figure 12.

The longitudinal accelerations for the no-strut model are presented in figure 13. The highest longitudinal acceleration obtained with this model was 33g at a horizontal velocity of 30 ft/sec and a negative impact attitude of 4°. The motions of the no-strut model were similar to those of the strut model with longitudinal acceleration reversals occurring at positive impact attitudes. The minimum time for reversal of the peak longitudinal accelerations was approximately 0.003 sec (0.006 sec full-scale) which occurred at a horizontal velocity of 15 ft/sec and a positive impact attitude of 2°. These accelerations ranged from -8g to +5g.

Acceleration Histories

Presented in figure 14 are acceleration traces obtained for the strut model at horizontal velocities of 0 and 50 ft/sec and impact attitude of 0°. The maximum normal acceleration onset rates were approximately 4900 and 4300g/sec for these two velocities, respectively. A slight lag can be noted in figure 14 between the peak longitudinal g and the peak normal g. This was caused by a slight horizontal movement of the heat shield before the honeycomb struts began to stroke.

Presented in figure 15 are acceleration traces obtained with the no-strut model at horizontal velocities of 0 and 50 ft/sec at an impact pitch attitude of 0°. The onset rates were found to vary greatly, with a maximum value of 38 000g/sec obtained in a normal acceleration at zero horizontal velocity.

Stability

The strut model was more stable than the no-strut model during slideout. The model was sufficiently stable that it did not turn over at impact pitch attitudes from -20° to +10° throughout the range of equivalent horizontal velocities of 0 to 50 ft/sec. The turnover conditions for the strut model are presented in figures 8, 10, and 12 by crossed points. The angular accelerations recorded with the strut model, as shown in figure 8, were found to be comparatively lower than those obtained with the no-strut model.

In comparison with the strut model, the no-strut model was less stable and the angular accelerations, illustrated in figure 9, were considerably higher. The no-strut model was stable through a range of negative pitch attitudes throughout the range of equivalent horizontal velocities of 0 to 50 ft/sec. Tumble in stability was apparent with this model at positive pitch attitudes and the strut model exhibited an increased stability margin at a positive pitch attitude of

approximately 10° at comparative horizontal velocities. The unstable conditions are illustrated in figures 9, 11, and 13 by the crossed points.

At a positive pitch impact attitudes, the center of gravity on both the strut model and the no-strut model was situated relatively high and well forward of the point of contact. This caused the models to pitch forward with appreciable angular accelerations. In the case of the strut model, two of the vertical struts were situated near the point of initial contact which resulted in a reduction of the vertical accelerations and consequently the angular accelerations. The additional four vertical struts were situated along the forward edge of the heat shield resulting in further attenuation of the angular accelerations. The net effect of the struts on the stability of the model was to allow an additional 10° positive pitch at the maximum horizontal velocity before the model became unstable and turned over.

REMARKS

The strut model data is felt to be closely representative of what should be expected from a full-scale vehicle employing a similar impact attenuation system since a major part of the impact energy is designed to be absorbed by the struts both in model and full-scale. The no-strut model accelerations are higher than expected from a full-scale vehicle because the model experienced very little strain and no structural failure, both of which could be expected from the full-scale spacecraft; however, this failure is difficult to design and to obtain repeatability. The development and qualification impact test program of a system depending on structural failure would be extensive and would require spacecraft structure. The scale effect of the soil may cause some variation in the results which would be obtained from the full-scale vehicle, however, this effect is felt to be small. The significant variation which can be expected will result from the fact that the models were tested on dry Ottawa Testing Sand, which is not representative of the type of terrain upon which the vehicle would be expected to impact. This sand was chosen for testing to provide a standard condition as near as possible to the actual conditions, which could be readily duplicated, and also which would minimize the possibility of damaging the no-strut model. Typical slideouts and depressions of the two models are shown in figure 16. It is interesting to note that the no-strut model under all conditions tested caused larger impact depressions and longer slideouts than the strut model. This occurred because the strut model was able to absorb some of its vertical and horizontal energy through its struts, whereas, with the no-strut

model all the energy had to be absorbed by the sand causing more of a depression and longer slideouts to dissipate its impact energy.

CONCLUSIONS

The following conclusions can be drawn from the data obtained in this program:

1. The model incorporating the strut system demonstrated a noticeably higher degree of impact stability than the model with no impact attenuation system. At negative impact attitudes, both the strut model and the no-strut model proved to be stable over the full range of horizontal velocities (up to 50 ft/sec) used in the tests. At positive pitch attitudes, the no-strut model was unstable at approximately 10° lower pitch attitudes than the strut model at corresponding horizontal velocities. It can be expected that under the same test conditions, the same relationship should exist between full-scale vehicles.

2. In general, the acceleration data obtained from the no-strut model were considerably more scattered and less predictable than the data obtained from the strut model. The data scatter would make it much more difficult to correlate the no-strut model data with a similar full-scale vehicle because the full-scale vehicle would experience structural failure. Such a failure is difficult to design and to obtain repeatability. Testing of a full-scale no-strut system would be extensive and require spacecraft structure. The strut model data with a full-scale vehicle with a similar impact attenuation system would be comparative because the major portion of the impact energy is absorbed by the attenuation struts both for model and full-scale design. Development and qualification testing would not require spacecraft structure except for system demonstration.

3. The peak angular accelerations experienced by the no-strut model were greater than those of the strut model by a factor of 3.1.

4. The peak normal accelerations experienced by the no-strut model were greater than those of the strut model by a factor of 5.6.

5. The peak longitudinal accelerations experienced by the no-strut model were greater than those of the strut model by a factor of 1.7.

REFERENCES

1. Bennett, R. V.: One-quarter Scale Apollo Impact Attenuation Model, Report No. NA62H-513, 1962.

2. Benson, Harold E.: Project Apollo Landing Characteristics of an Apollo-Type Vehicle, Working Paper No. 1039, 1961.

3. Blanchard, Ulysse J.: Landing Characteristics of a Lenticular-Shaped Reentry Vehicle, NASA TN D-940, 1961.

TABLE I.- COMPARATIVE DIMENSIONS OF ONE-QUARTER SCALE MODELS AND FULL-SCALE VEHICLE

	No Strut Model/Full-Scale	Strut Model/Full-Scale
Total Weight, lb.	117.5/7520	114.5/7328
Moment of Inertia (approx)		
Roll, Slugs - ft^2	3.54/3630	3.823/3915
Pitch, slugs - ft^2	2.629/2700	3.366/3440
Yaw, slugs - ft^2	2.82/2890	2.094/3447

SCALE RELATIONSHIPS

(τ = Scale of Model)

Quantity	Full-Scale	Scale Factor	Model
Length	l	τ	τ l
Area	A	τ^2	τ^2 A
Weight	W	τ^3	τ^3 W
Moment of inertia	I	τ^5	τ^5 I
Time	t	$\sqrt{\tau}$	$\sqrt{\tau}$ t
Velocity	v	$\sqrt{\tau}$	$\sqrt{\tau}$ v
Linear acceleration	a	1	a
Angular acceleration	α	τ^{-1}	τ^{-1} α
Force	F	τ^3	τ^3 F

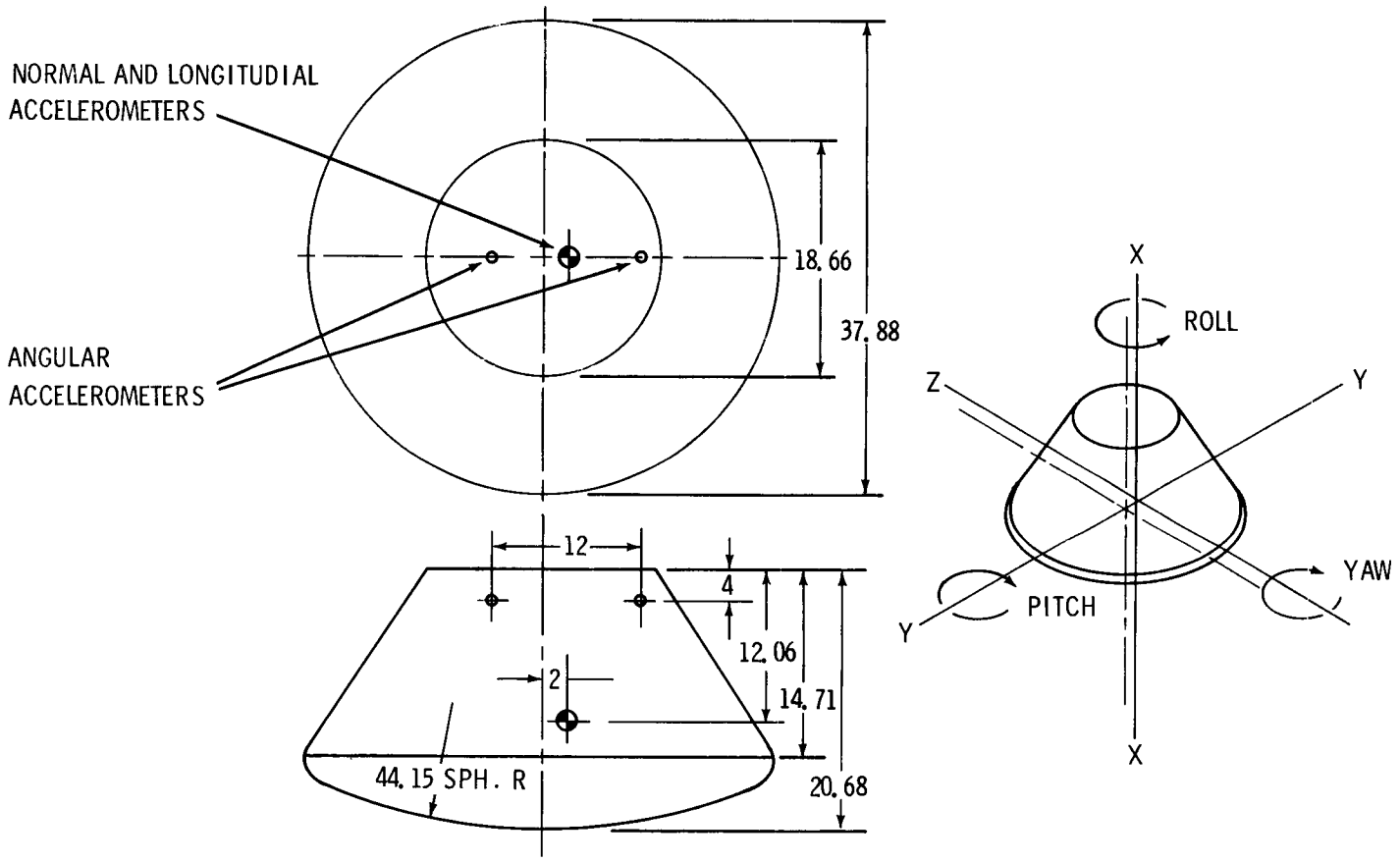

Figure 1.- General arrangement of one-quarter scale dynamic Apollo model with no impact attenuation struts.

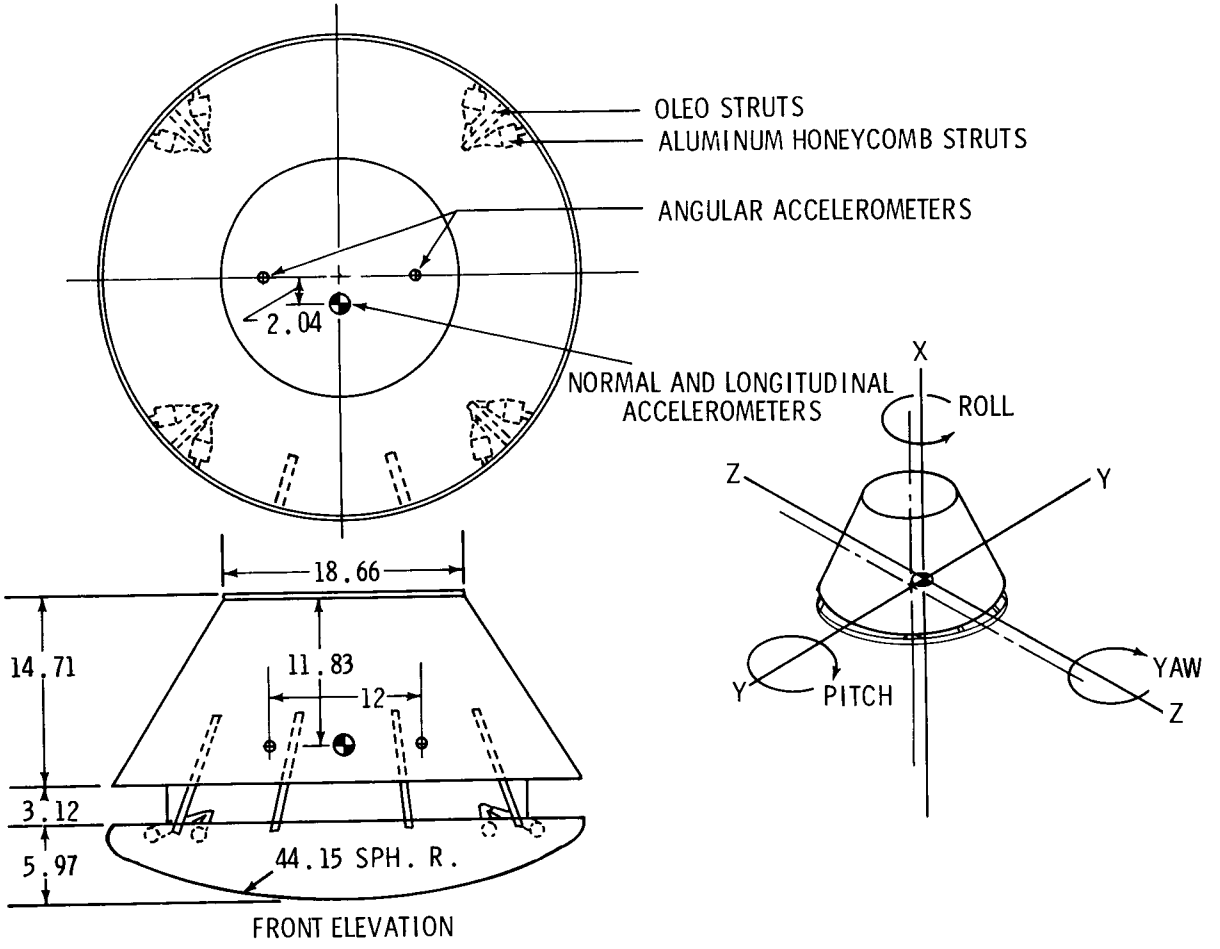

Figure 2.- General arrangement of one-quarter-scale dynamic Apollo model incorporating impact attenuation struts.

NASA-S-65-705

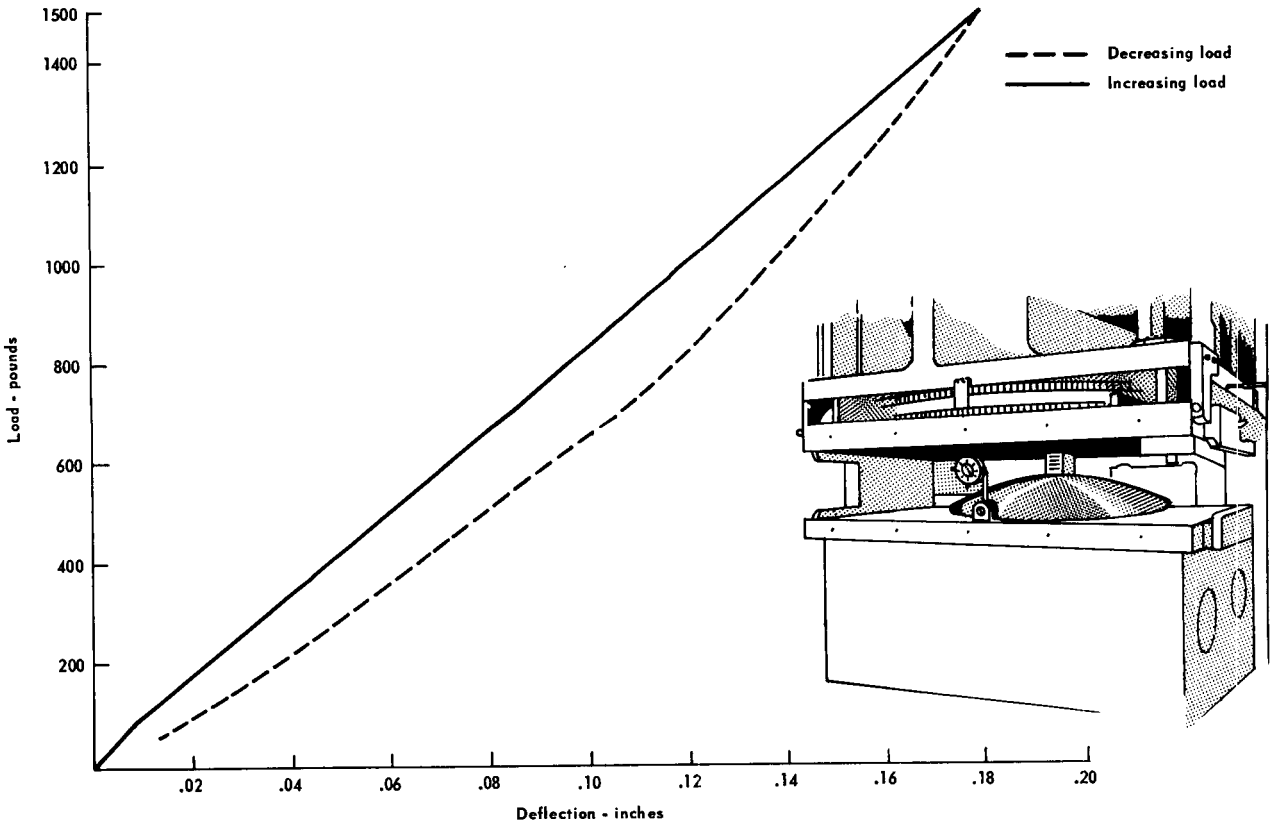

Figure 3.- Heat shield force-deflection and test setup.

NASA-S-65-699

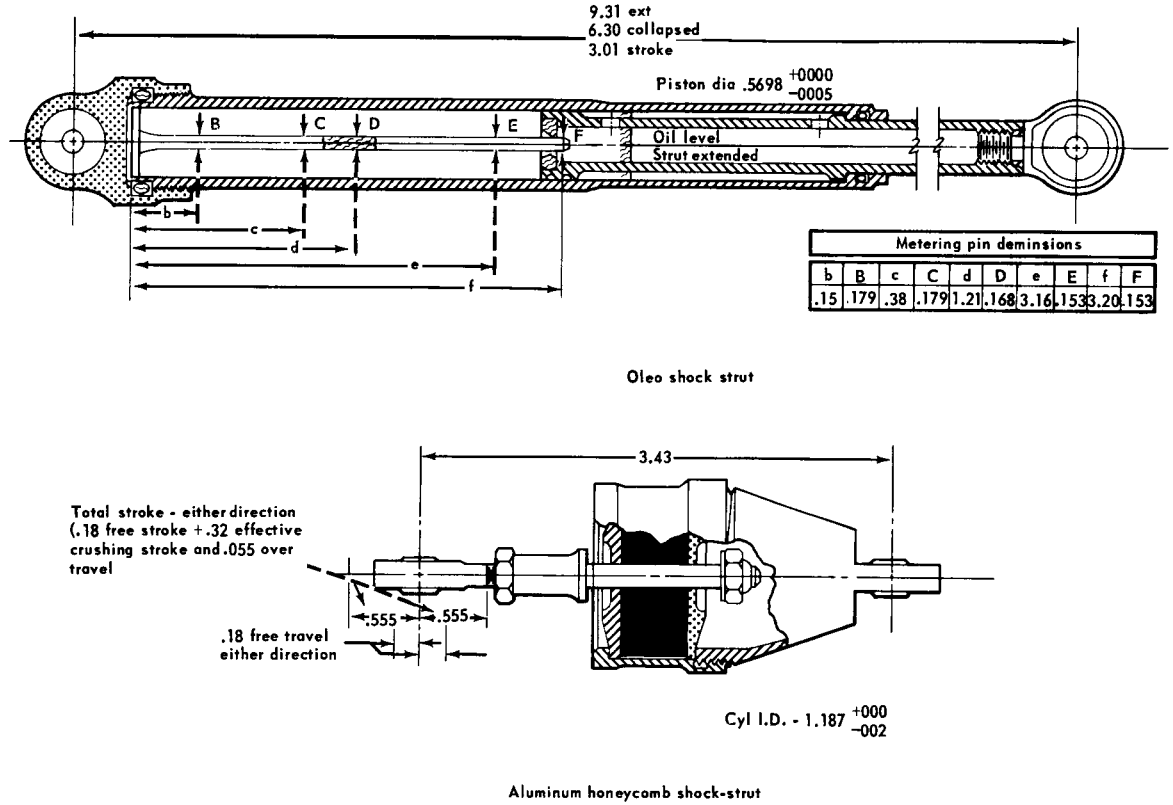

Figure 4.- Sketches of vertical and horizontal shock struts.

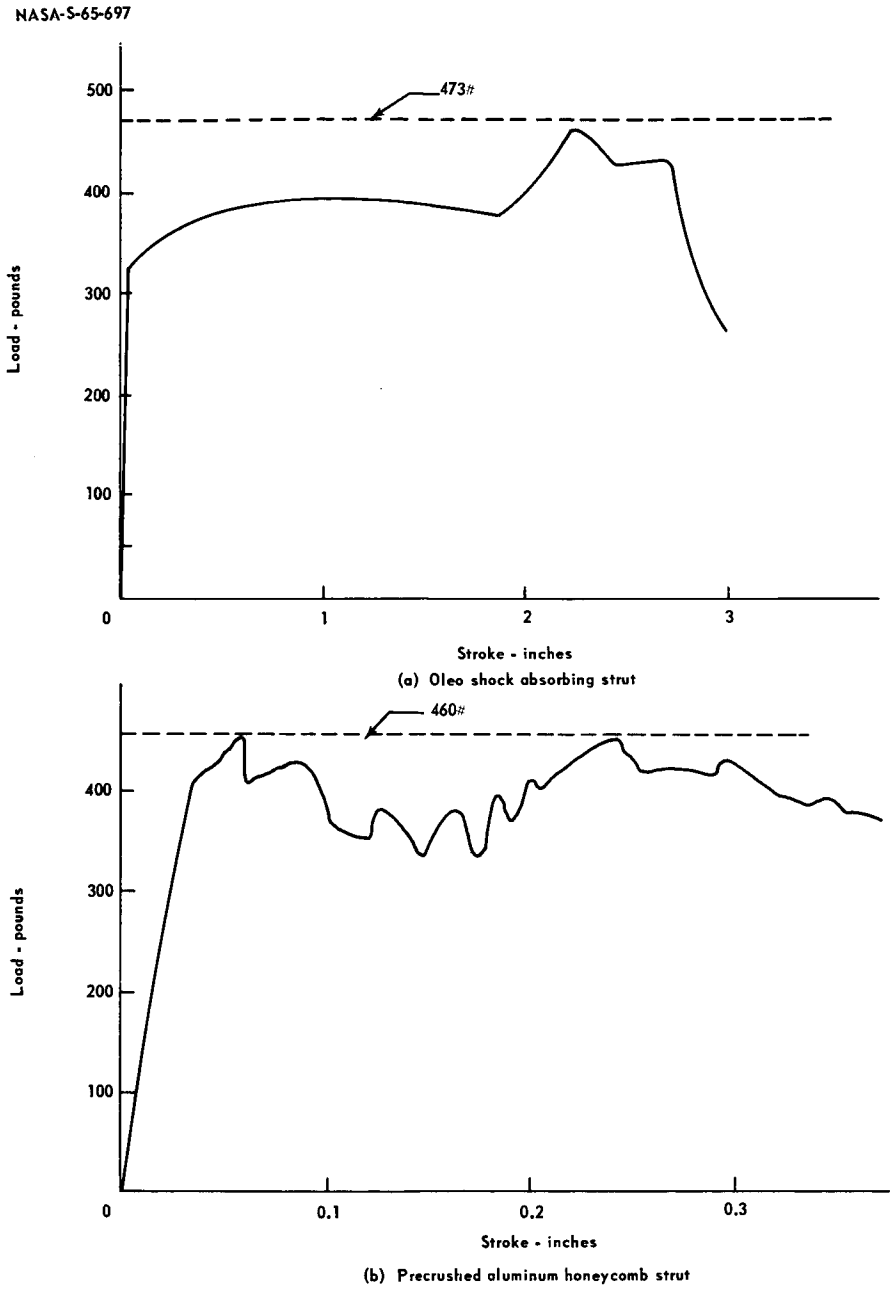

Figure 5.- Force-deflection curves for the oleo and honeycomb struts.

NASA-S-65-696

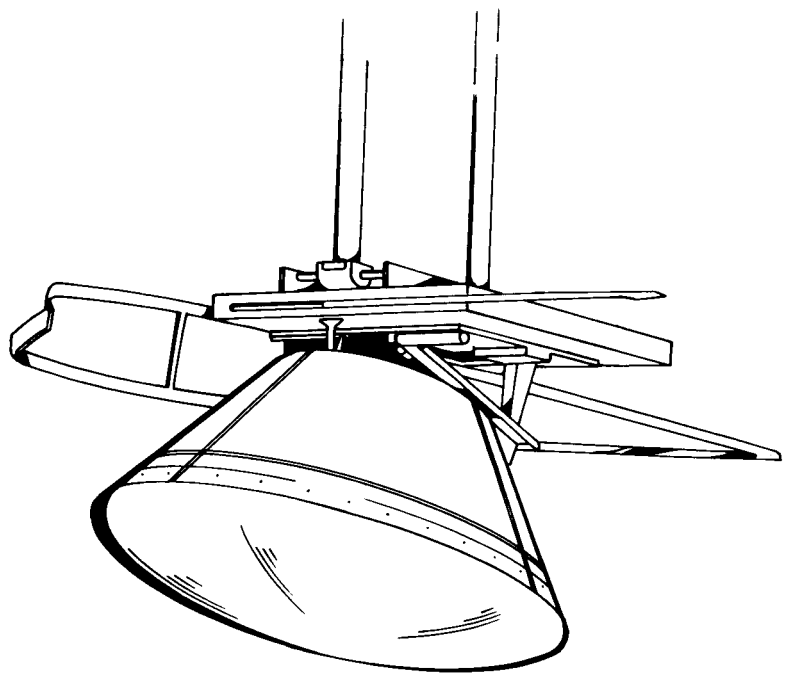

Figure 6.- Model on support carriage.

NASA-S-65-704

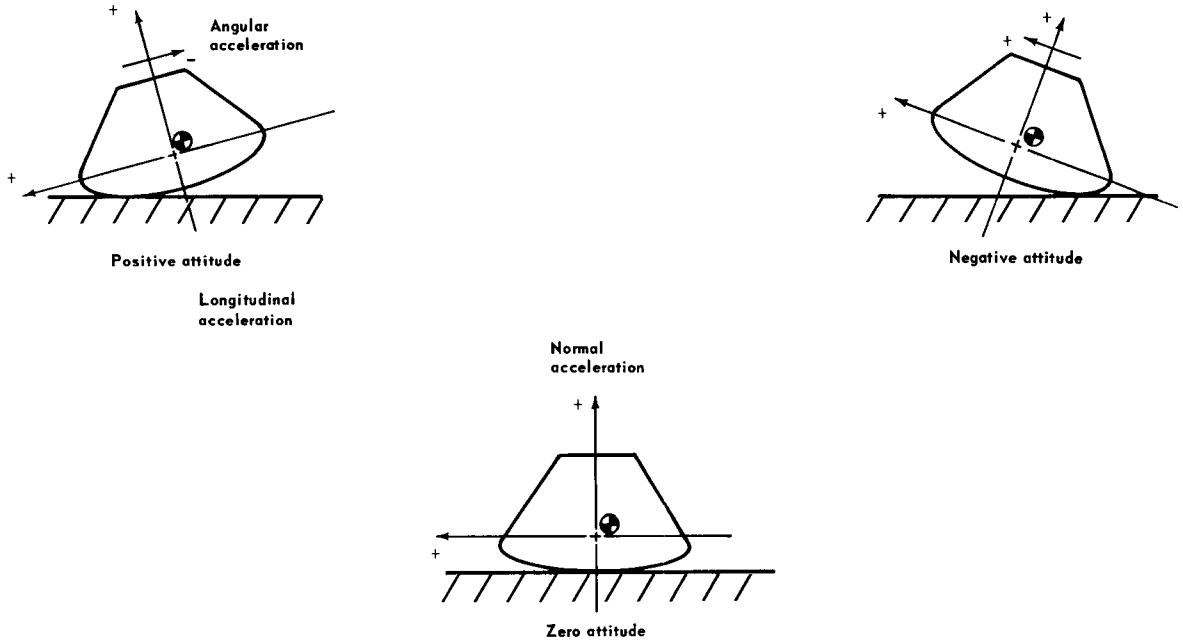

Figure 7.- Definition of axes, accelerations and attitudes.

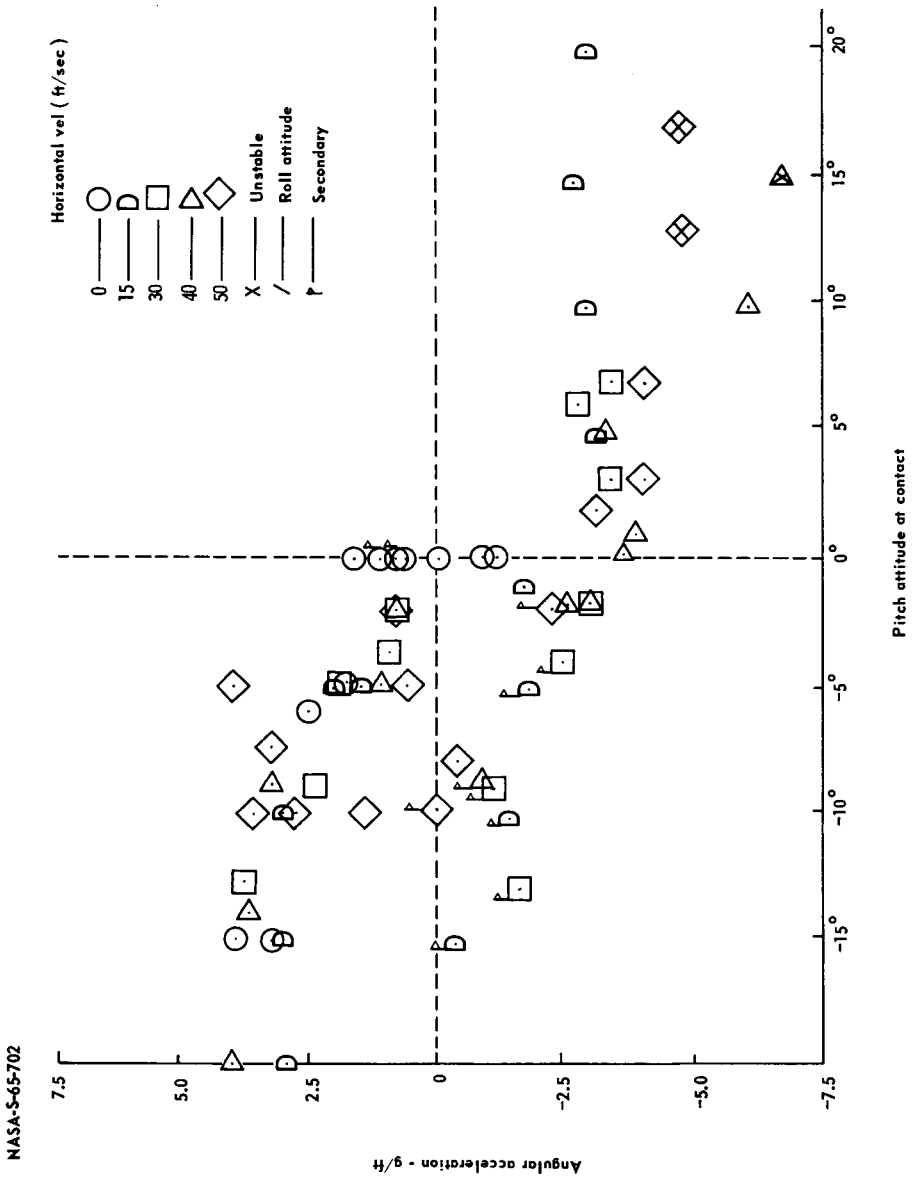

Figure 8.- Strut model angular accelerations.

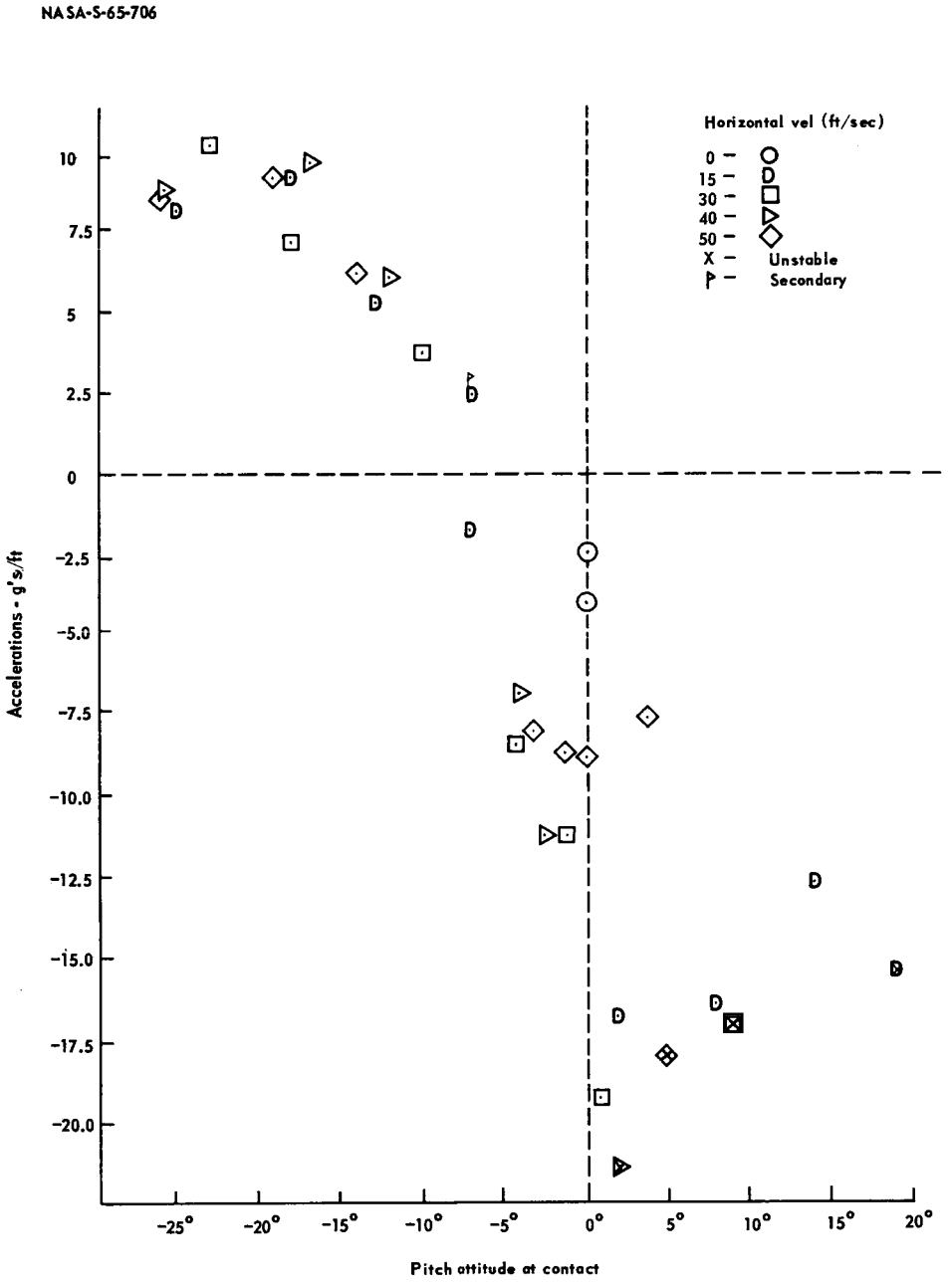

Figure 9.- No strut model angular accelerations.

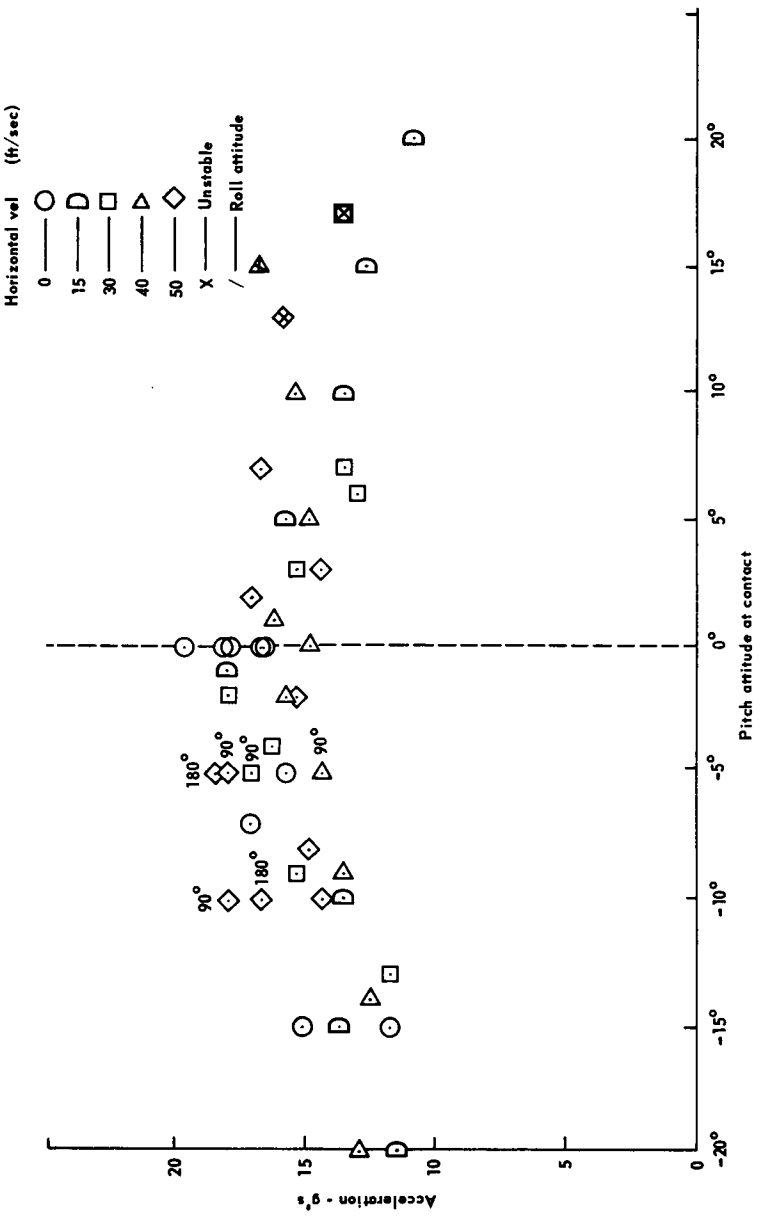

NASA-S-65-707

Figure 10.- Strut model normal accelerations.

NASA-S-65-701

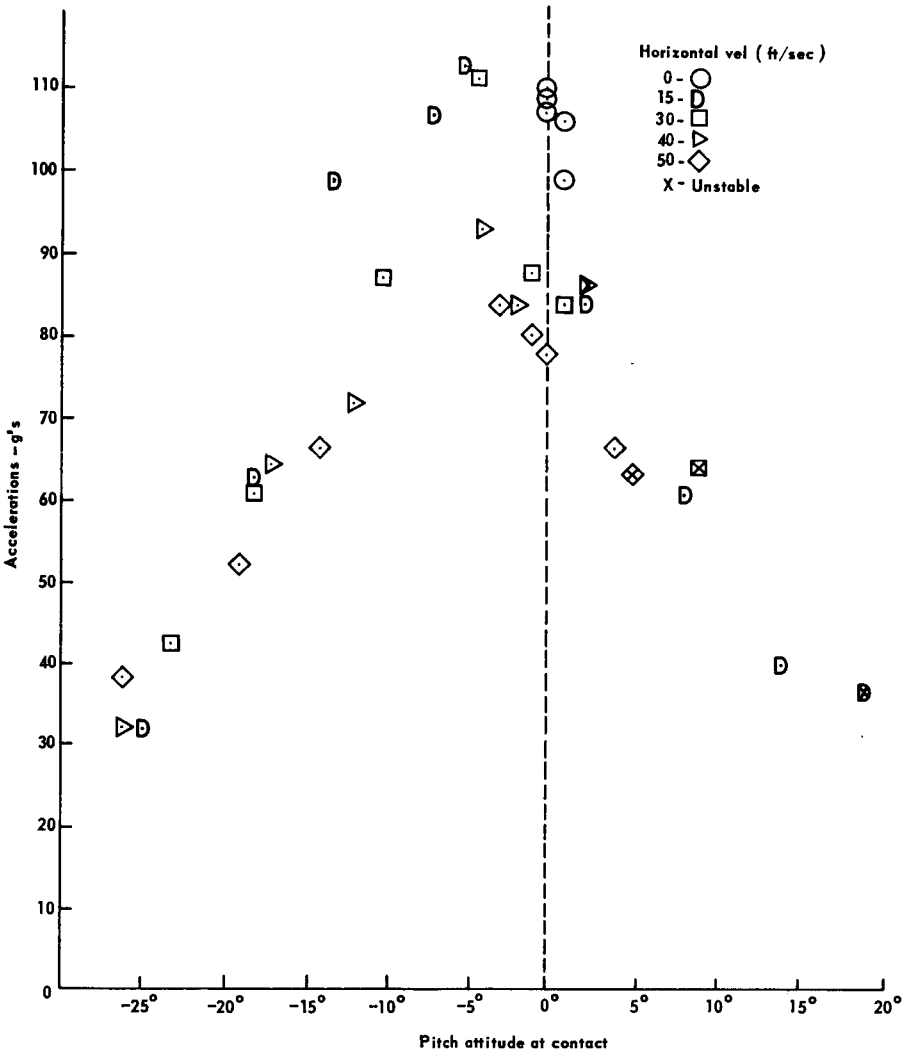

Figure 11.- No strut model normal accelerations.

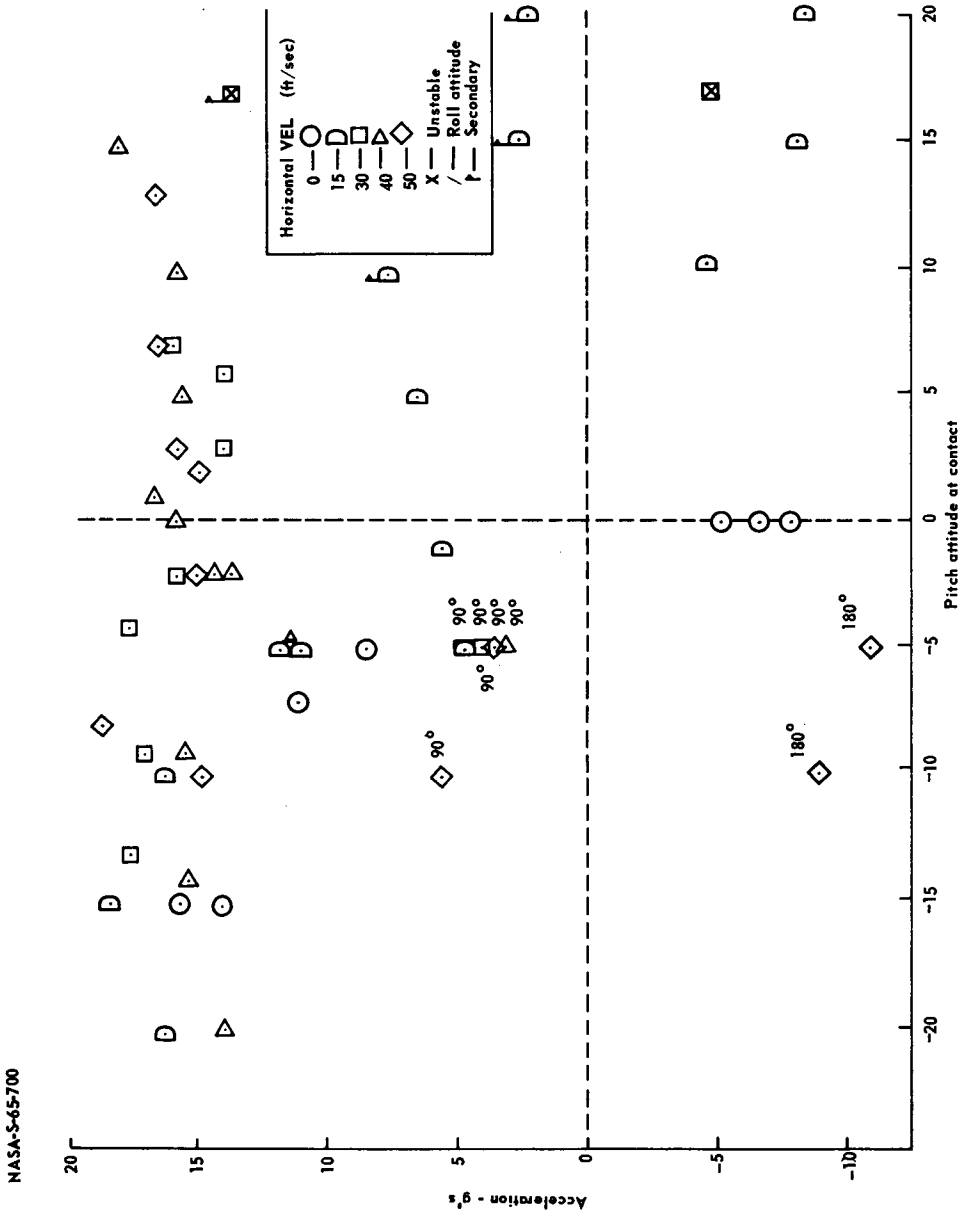

Figure 12.- Strut model longitudinal accelerations.

NASA-S-65-694

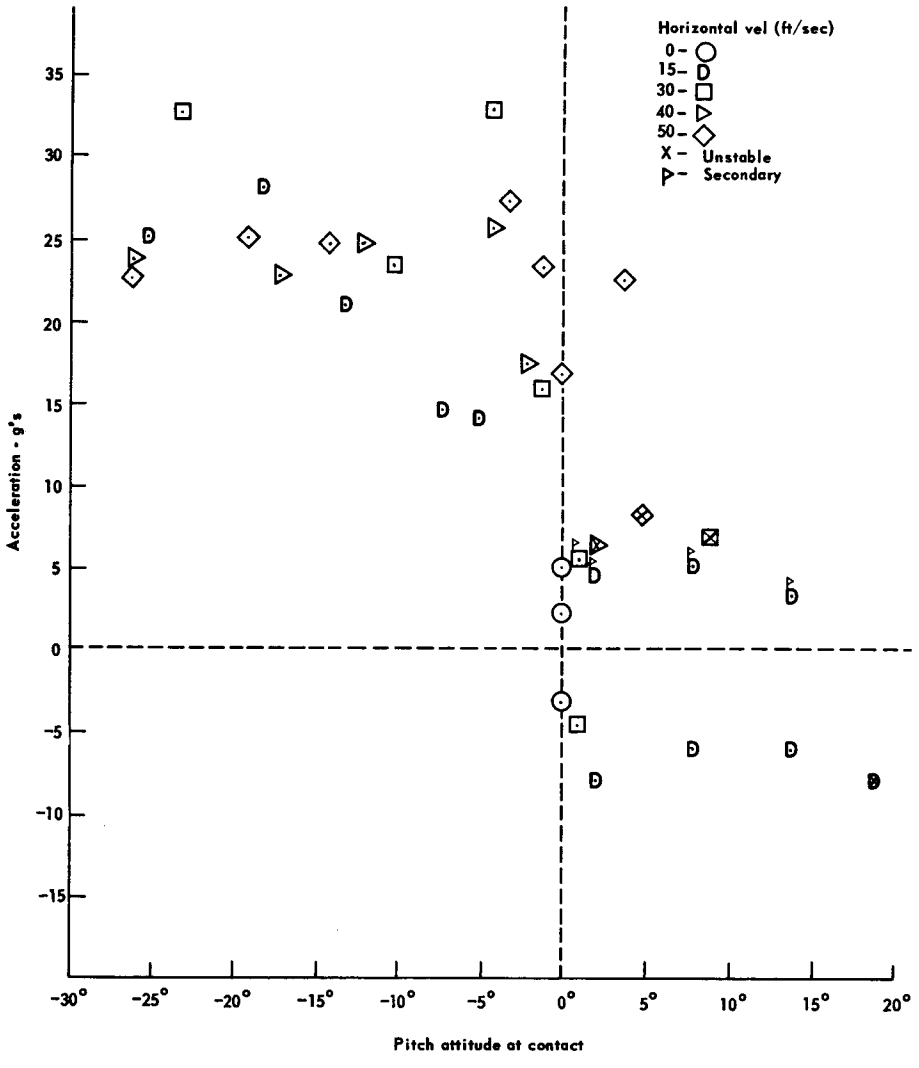

Figure 13.- No strut model longitudinal accelerations.

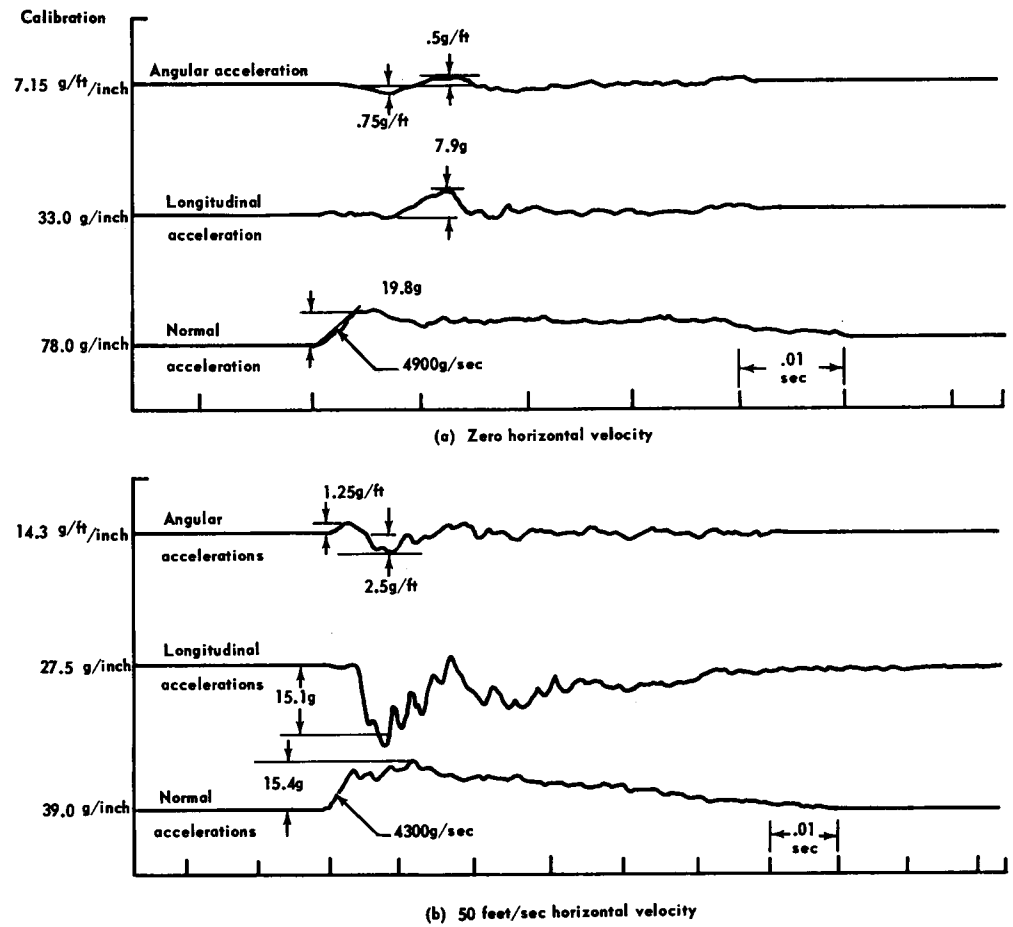

Figure 14.- Typical acceleration histories for strut model.

NASA-S-65-698

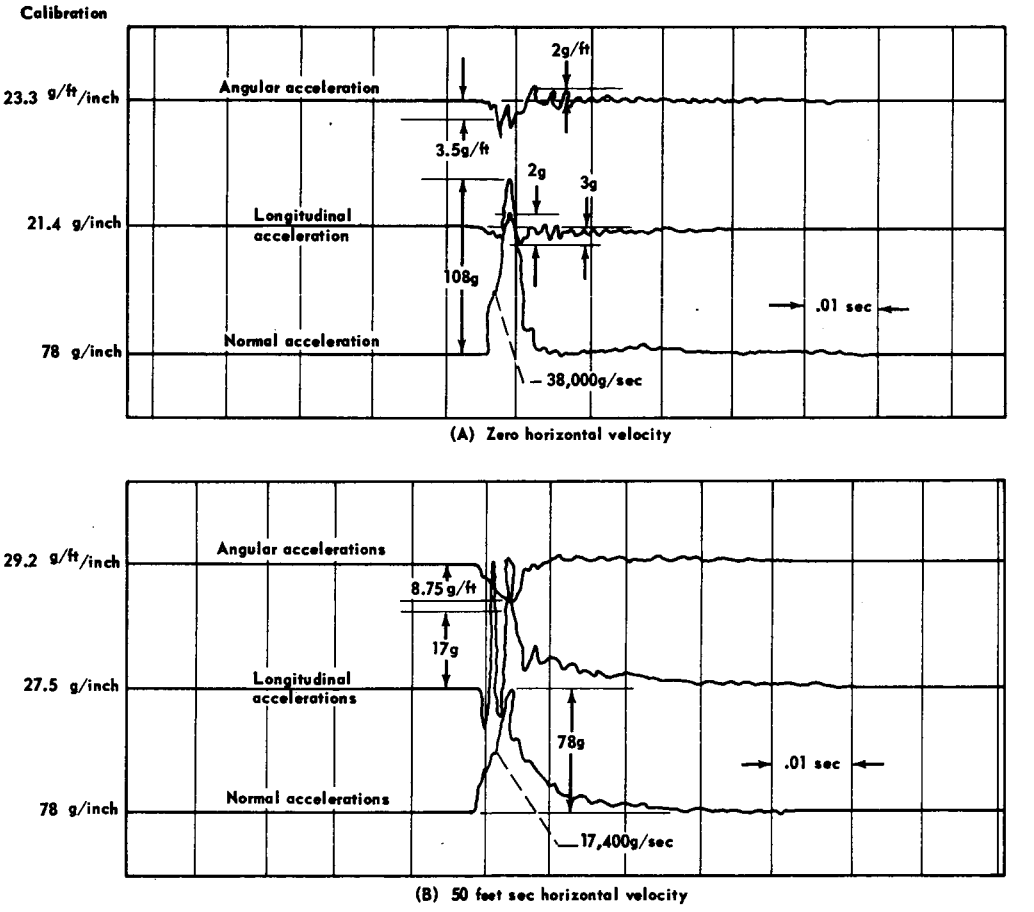

Figure 15.- Typical acceleration histories for the no strut model.

NASA-S-65-703

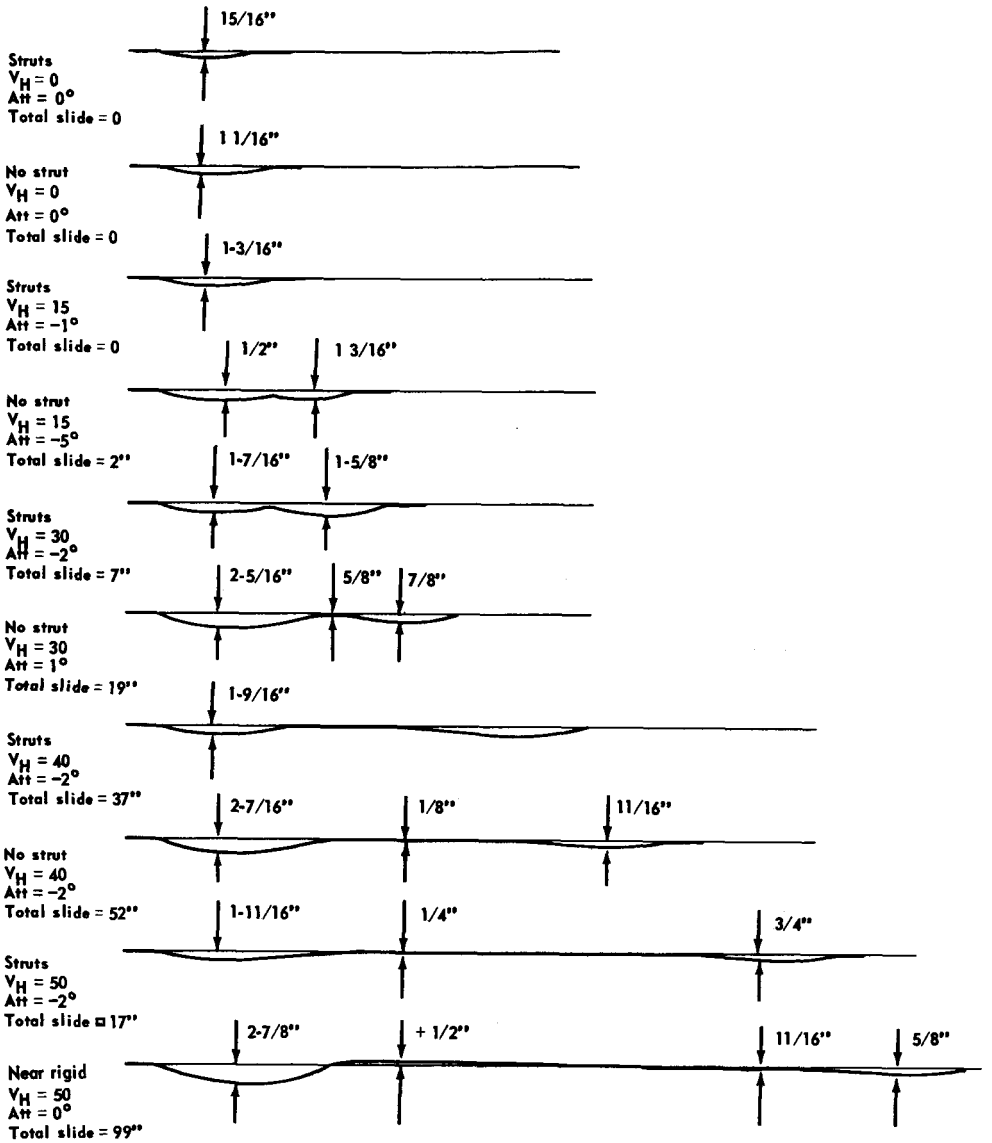

Note: Vertical component of velocity constant at 30 fps

Figure 16.- Typical impact depressions.